journal

J. Am. Ceram. Soc., 76 [12] 3029–33 (1993)

Shape Evolution of a Coherent Tetragonal Precipitate in Partially Stabilized Cubic ZrO_2: A Computer Simulation

Yunzhi Wang,*,† Hongying Wang,† Long-Qing Chen,*,‡ and A. G. Khachaturyan†

Department of Materials Science and Engineering, Rutgers University, Piscataway, New Jersey 08855-0909

Department of Materials Science and Engineering, Pennsylvania State University, University Park, Pennsylvania 16802

The kinetics of shape evolution of a tetragonal precipitate coherently embedded in a cubic matrix are examined. Specifically, the morphology of tetragonal ZrO_2 particles in partially stabilized cubic ZrO_2 is discussed. A computer simulation, carried out without any a priori constraint on possible kinetic paths and particle morphologies, shows that a lenslike shape appears during *growth* of a tetragonal particle. Upon further *coarsening*, the shape relaxes into a rhombus bounded by facets. Depending on the balance between interfacial and strain energies controlled by the particle size, the facets can be smoothly curved or straight. The predicted particle morphologies are in good agreement with the experimental observations. The kinetic model proposed is quite general for simulating microstructural developments during decomposition involving a crystal lattice symmetry change where elastic strain accommodation plays an important role.

I. Introduction

THE discovery of transformation-toughening behavior in partially stabilized zirconia (PSZ) has generated enormous research activities on the phase equilibria and microstructural development in ZrO_2 and related systems (see, for example, reviews by Stubican,[1] Heuer,[2] and Cannon[3]). In particular, the precipitation kinetics of the tetragonal (t-) ZrO_2 particles from the cubic (c-) ZrO_2 matrix, which control the shape, size, and spatial distribution of the tetragonal particles and hence determine mechanical properties of the material, have been extensively studied[4–12] (see the reviews[2,3] for additional references).

The morphology of the t-ZrO_2 particles in Mg-PSZ was originally characterized as ellipsoidal.[4,5] Later the tilting TEM experiment[7] demonstrated that the precipitates have a lenslike rather than ellipsoidal shape. A close edge-on examination by Ruhle and Kriven[8] revealed that the precipitates very often have a faceted morphology with straight interfaces and sharp corners. Recently, a TEM study of the microstructural evolution in Mg and Mg-Y PSZs at longer aging times was performed by Bateman and Notis.[12] They observed a gradual transition of a lenslike morphology formed at the beginning of aging into a faceted one at later stages of aging. Since particles of different morphologies generate different stress fields and hence behave differently in the stress-induced martensitic transformation, factors controlling a shape evolution of the t-ZrO_2 particles are very important.

It has been first indicated by Lanteri *et al.*[11] that a faceted morphology of the t-ZrO_2 in Mg-PSZ could be associated with accommodation of the coherent strain generated by the crystal lattice misfit between the t-phase precipitate and the c-phase matrix. They assumed that the orientation of the facets is the same as that of habit planes of a thin platelike coherent precipitate. Then they calculated the habit plane orientation by minimizing the strain energy according to Khachaturyan's theory.[13] Similar results were obtained in Ref. 12, where the precipitate shape was approximated to a circular disk with a finite aspect ratio. Although these assumptions do not correspond to the observed particle shapes in Mg-PSZ (the particles do not usually have a platelike morphology), there is a very good agreement between the predicted and observed facet orientations. This raises a question about the limits of applicability of this approach. To answer the question, a more general and accurate theory should be used which would not pose any constraints on possible optimal particle shapes and would take into account the interfacial energy as well as the strain energy. It would also be interesting to investigate not only the energetic but also the kinetic aspect of the particle shape transformation and, particularly, to find sequences of transient particle shape formation at different stages of decomposition.

It is the purpose of this paper to formulate such a general approach and apply it to study the kinetics of shape evolution of a t-phase particle coherently embedded in a c-matrix. To avoid any a priori constraints on the possible particle morphologies and transformation paths, a kinetic field model based on the Ginzburg–Landau (GL) phenomenological theory was employed. Different from the conventional approach where the particle morphology is characterized by the geometry of the interfacial boundaries between two strictly distinctive phases with fixed structures, this model characterizes the morphology and its evolution by coordinate-dependent continuous fields of concentration and long-range order (lro) parameters. The structure transformation kinetics are described by the temporal evolution of these fields determined from a solution of the nonlinear time-dependent Ginzburg-Landau (TDGL) equations. Review of the applications of the GL theory to first-order phase transformations has been given by Gunton *et al.*[14]

In this paper we advance the theory of incorporating the transformation-induced coherent elastic strain into the TDGL equations by adding the strain energy functional[13,15] to the total free energy in the driving force. This makes the theory applicable to the most interesting and technologically important cases, where the phase transformations result in substantial crystal lattice rearrangements and symmetry changes. The theory[13] provides a mathematical framework for calculating the strain energy of a precipitate of arbitrary geometry. However, this calculation cannot be done analytically. Therefore, a computer simulation technique has been used. The main advantage of the proposed technique is that the nonlinear TDGL equations automatically take care of all complications caused by the self-consistent boundary conditions on the moving interfaces. In

P. K. Davies—contributing editor

Manuscript No. 194503. Received June 4, 1993; approved August 3, 1993.

Supported by the National Science Foundation under Grant No. NSF-DMR-9123167. The simulation was performed on a Cray-C90 at Pittsburgh Supercomputing Center under Grant No. DMR900043P.

†Rutgers University.

‡Pennsylvania State University.

*Member, American Ceramic Society.

principle, it is able to describe an arbitrary morphology of a multiparticle coherent system and its temporal evolution during decomposition.

In the computer simulation, the materials constants of Mg-PSZ are used to fit the GL free-energy model, so the results are valid for the microstructural developments of the tetragonal particles in Mg-PSZ. We first focus on a single particle problem, which represents a case where a typical separation between the precipitates is much greater than the typical particle size. It enables us to investigate the evolution of particle shape and orientation excluding the multiparticle effect, the effect caused by the combined strain field generated by all the other precipitates presented in the crystal. Then the possible multiparticle effect is illustrated by a particular case of two interacting particles. The characteristic behaviors of particle shape transformation and spatial pattern formation in a dense multiparticle system, where the interactions between particles play an important role, will be presented in a separate paper.

II. Kinetic Model and Simulation Procedure

The PSZ is a cubic solid solution with the fluorite structure at high temperatures. It decomposes into a coherent mixture of a solute (Mg, CaO, or Y_2O_3)-rich cubic and a solute-poor tetragonal phase when quenched into a two-phase region of the phase diagram. Since a cubic $\longrightarrow$ tetragonal phase transformation is accompanied by a point group symmetry reduction, there are three orientation variants or domains of the product t-phase. To fully describe the morphology, we need three lro parameters, e.g., η_1, η_2 and η_3. In the case of PSZ they are the amplitudes of symmetry breaking "soft" optical displacive modes. The stress-free "coarse grain" free energy F_c (which does not include the transformation-induced strain) is then a functional of the concentration field $c(\mathbf{r})$ and lro parameter fields $\eta_j(\mathbf{r})$, i.e.,

$$F_c = F_c[c(\mathbf{r}), \eta_1(\mathbf{r}), \eta_2(\mathbf{r}), \eta_3(\mathbf{r})]$$

In this paper we consider only particles belonging to the same orientation variant, i.e., a situation where $\eta_1(\mathbf{r}) = \eta(\mathbf{r})$, $\eta_2(\mathbf{r}) = \eta_3(\mathbf{r}) = 0$. The specific stress-free free energy at a given temperature can be approximated by the Landau free-energy polynomial

$$f(c,\eta) = \frac{1}{2}A(c - c')^2 - \frac{1}{2}B\eta^2 - \frac{1}{4}C\eta^4 + \frac{1}{6}D\eta^6 + \frac{1}{2}Gc\eta^2 \quad (1)$$

where A, B, C, D, and G are positive constants and c' is a constant close to the equilibrium composition of the cubic phase. The last term in Eq. (1) describes the coupling between the concentration and lro parameter. The constants are chosen in such a way that they provide the free-energy topology required for the system in a two-phase field of the phase diagram. A particular case characterized by the constants $A = 80$, $B = 0.8$, $C = 0.5$, $D = 0.14$, and $G = 5$ in Eq. (1) is chosen (all the energies involved in the numerical calculation are measured in a unit $k_BT \sim 2 \times 10^9$ erg/cm^3). This choice provides equilibrium compositions $c_{tetr} = 0.045$ for the t-phase and $c_{cub} = 0.155$ for the c-phase, which are close to the equilibrium compositions of Mg-PSZ at 1420°C.[1] Minimizing the free energy (Eq. (1)) with respect to η at given c allows us to express the minimizing lro parameter through composition, i.e., $\eta = \eta_o(c)$, and thus exclude η from Eq. (1). The resultant function $f(c,\eta_o(c))$ is a projection of the free-energy minima with respect to η on the f–c plane. A typical dependence of $f(c,\eta_o(c))$ on c is shown in Fig. 1 for the given set of parameters A, B, C, D, and G. As expected, the free energy has two branches: one of them describes the t-phase ($\eta = \eta_o$) while the other describes the c-phase ($\eta = 0$). Their common tangent determines the equilibrium compositions of the t- and c-phase at the stress-free state. With Eq. (1), the stress-free, free-energy functional F_c of the functions $c(\mathbf{r})$ and $\eta(\mathbf{r})$ becomes

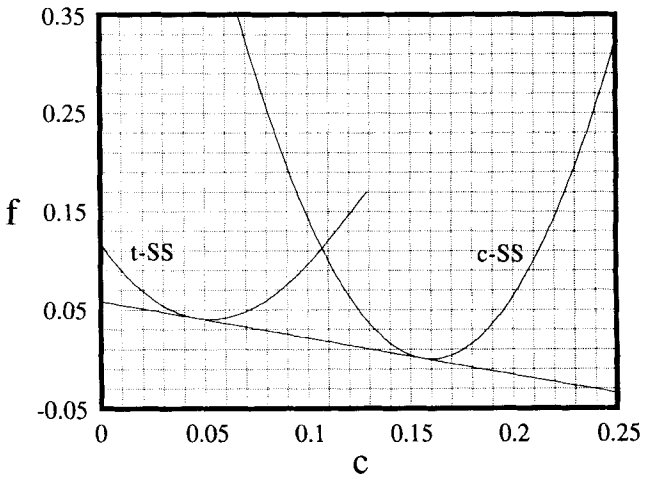

Fig. 1. Specific free-energy vs composition curves for both the tetragonal and cubic solid solutions calculated according to Eq. (1) with $\eta = \eta_o(c)$ and $A = 80.0$, $B = 0.8$, $C = 0.5$, $D = 0.14$, $G = 5.0$. See text for explanation.

$$F_c = \int d\mathbf{r}\left[\frac{1}{2}\alpha|\nabla c|^2 + \frac{1}{2}\beta|\nabla\eta|^2 + f(c,\eta)\right] \quad (2)$$

where α and β are gradient coefficients. A constant gradient coefficient gives an isotropic interfacial energy.

The coupling between the strain field $\varepsilon_{ij}(\mathbf{r})$, where i and j are Cartesian indexes and the lro parameter field $\eta(\mathbf{r})$ is described by the first nonvanishing term in the free-energy expansion with respect to these fields. It is characterized by the stress-free transformation strain $\varepsilon^0_{ij}(\mathbf{r})$ responsible for the crystal lattice mismatch between the t-precipitate and the c-matrix. The stress-free transformation strain ε^0_{ij} and the lro parameter η are related as

$$\varepsilon^0_{ij}(\mathbf{r}) = \varepsilon^{00}_{ij}\frac{\eta^2(\mathbf{r})}{\eta_0^2(c_{tetr})} \quad (3)$$

where $\eta_o(c_{tetr})$ and ε^{00}_{ij} are the lro parameter and stress-free transformation strain of the equilibrium tetragonal phase, respectively. If we assume that the matrix and precipitate have the same elastic moduli, the total strain energy functional of an arbitrary lro parameter field may be presented in the reciprocal space in a close form:[15]

$$E_{el} = \frac{1}{2}\int\frac{d^3k}{(2\pi)^3}B(\mathbf{n})|\{\eta^2(\mathbf{r})\}_k|^2 \quad (4)$$

where

$$B(\mathbf{n}) = c_{ijkl}\varepsilon^{00}_{ij}\varepsilon^{00}_{kl} - n_i\sigma^0_{ij}\Omega_{jk}(\mathbf{n})\sigma^0_{kl}n_l \quad (5)$$

c_{ijkl} is the elastic constant tensor, $\sigma^0_{ij} = c_{ijkl}\varepsilon^{00}_{kl}$, $\mathbf{n} = \mathbf{k}/k$ is a unit vector in the reciprocal space and n_i is the ith component of $\mathbf{n}$, $\Omega_{jk}(\mathbf{n})$ is a Green function matrix reciprocal to $\Omega^{-1}_{jk}(\mathbf{n}) = c_{ijkl}n_in_l$, and

$$\{\eta^2(\mathbf{r})\}_k = \int\eta^2(\mathbf{r})e^{-ikr}d^3r$$

The singular branching point $\mathbf{k} = 0$ is excluded from the integration in Eq. (4).

The nonlinear continuum TDGL equations for the concentration and lro parameter fields have the following forms:

$$\frac{dc(\mathbf{r},t)}{dt} = M\nabla^2\frac{\delta F}{\delta c(\mathbf{r},t)} \quad (6a)$$

$$\frac{d\eta(\mathbf{r},t)}{dt} = -L\frac{\delta F}{\delta\eta(\mathbf{r},t)} \quad (6b)$$

where M and L are material constants characterizing the diffusional mobility and lro kinetics, respectively, and $F = F_c + E_{el}$ is the total free energy including the strain energy contribution. The variational derivatives $\delta F/\delta c(\mathbf{r},t)$ and $\delta F/\delta \eta(\mathbf{r},t)$ are the thermodynamic driving forces for the relaxation of $c(\mathbf{r},t)$ and $\eta(\mathbf{r},t)$, which actually contain all the information about the microstructural evolution.

Using Eqs. (2) and (4), we solve the coupled Eqs. (6*a*) and (6*b*) numerically in the reciprocal space. Although the kinetic model is formulated in a three-dimensional space, we use at this stage a two-dimensional (2D) model system to save the computational time. It is equivalent to an assumption that all the considered particles are cylinders (of arbitrary-shaped cross section) perpendicular to the 2D plane. A computational cell of 256 × 256 grids is considered. Periodic boundary conditions are applied along both dimensions. The experimental data for the elastic constants and lattice parameters of Mg-ZrO_2 at 1420°C given in Ref. 12 are used. They are $c_{11} = 3.08 \times 10^{12}$ erg/cm^3, $c_{12} = 0.69 \times 10^{12}$ erg/cm^3, $c_{44} = 0.36 \times 10^{12}$ erg/cm^3, $a_c = 5.094$ Å, $a_t = 5.091$ Å, and $c_t = 5.204$ Å. The gradient coefficients α and β in Eq. (2) are assumed to be 0.2. Reduced time is used in the simulation, which is defined in a unit of typical relaxation time for the lro parameter, $t_o = (L k_B T)^{-1}$, i.e., $t^* = t/t_o$. The ratio of M/L is chosen to be 0.4.

III. Results and Discussion

After nucleation, the sequence of morphological evolution during decomposition can be divided into two stages: the growth, where the equilibrium compositions and volume fractions of coexisting phases are not yet attained, and coarsening, where the two-phase pattern rearrangement occurs at fixed total phase volumes and compositions under zero supersaturation. The difference between these two stages is that the driving force for the growth stage is determined by the volume-dependent free energies including the bulk "chemical" free energy and the strain energy, whereas the driving force for coarsening is determined by the morphology-dependent interfacial energy and the strain energy.

(1) Shape Evolution at Growth

The temporal shape evolution of the tetragonal precipitate during growth is shown in Figs. 2(a–d) in terms of the concentration field $c(\mathbf{r},t)$. It is simulated by an initial configuration consisting of a small equiaxed t-phase particle of equilibrium composition and lro parameter coherently embedded in a supersaturated c-phase matrix of composition 0.115 (Fig. 2(a)). In those figures and the following ones, completely dark regions represent $c(\mathbf{r},t) = c_{cub}$, which describes the equilibrium c-phase, while completely white ones represent $c(\mathbf{r},t) = c_{tetr}$, which describes the equilibrium t-phase. The c-axis of the t-phase particle is directed along the [01] vertical direction. The radius of the particle is equal to $8\Delta r$, where Δr is the length of the grid. To enlarge the tetragonal particle, only about 34% of the $256\Delta r \times 256\Delta r$ matrix which contains the tetragonal particle is shown in the pictures.

As the aging proceeds, a highly anisotropic growth is first observed (Fig. 2(b)). For example, the particle grows much faster along the [10] direction than the [01] direction that is parallel to the c-axis along which the lattice misfit is maximal. This anisotropic growth results in a lenslike particle shape. Further growth maintains this morphology; e.g., there is a self-similarity between the particle shapes shown in Figs. 2(c) and (d). However, if the supersaturation of the matrix vanishes (e.g., the growth stage is over and the particle undergoes coarsening), a gradual transformation from the lenslike shape (Fig. 2(d)) to a faceted morphology (Fig. 2(e)) occurs. This prediction is actually in a good agreement with the experimental observations by Bateman and Notis.[12] They have shown that in Y-Mg PSZ all particles have a lenslike shape at the beginning of aging (Fig. 2(b) in Ref. 12(a)) but most of them transform after 5 h of aging into a faceted morphology (Fig. 6 in Ref. 12). It can be readily seen from this simulation that a lenslike morphology is mostly associated with the particle growth kinetics.

(2) Shape Changes during Coarsening

To examine the equilibrium particle shape during coarsening, both the precipitate and matrix are assumed to have the equilibrium compositions and structures. We start from a circular

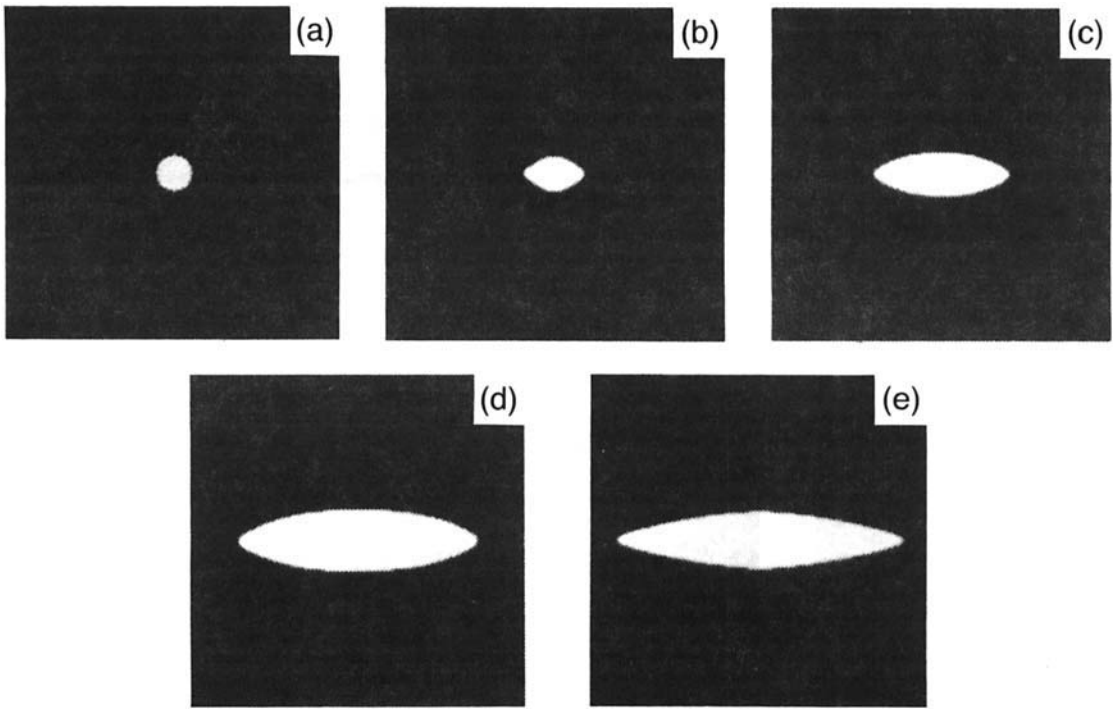

Fig. 2. (a–d) Temporal shape evolution during the growth of a tetragonal particle embedded in a supersaturated cubic matrix. About 34% of the computational cell is presented. (a–d) correspond to $t^* = 0$, 20, 80, and 160, respectively (see text for the definition of t^*). (e) Relaxed particle shape, developed from (d), after the supersaturation of the matrix vanishes.

t-phase particle of radius $30\Delta r$. The diffusional relaxation of the particle towards an equilibrium shape, determined by the balance between the interfacial and strain energies, is described by the coupled set of kinetic equations (*6a*) and (*6b*) for $c(\mathbf{r},t)$ and $\eta(\mathbf{r},t)$. The balance between the interfacial and strain energies which controls the equilibrium particle shape can be expressed through a ratio

$$\xi = \frac{E_s}{E_{el}} = \frac{r_0}{L} \tag{7}$$

where $r_0 = \gamma/\lambda\varepsilon_0^2$ (γ is the specific interfacial energy, and λ and ε_0 are the typical elastic modulus and typical stress-free transformation strain, respectively) is a material constant, and $L = V/S$ (V and S are the total volume and surface area of the particle, respectively) is a typical length scale of the particle. In 2D, $L = S/P$, where P is the perimeter of the 2D particle. Equation (7) follows from a fact that E_s is proportional to interfacial area, while E_{el} to volume. According to Eq. (7), there is a continuous decrease of ξ as a particle grows in size and, thus, the balance between the interfacial and strain energy shifts in the direction of increasing the strain energy. As a result, a change of the equilibrium particle shape should be expected. Since it is technically difficult to simulate a particle size growth due to coarsening (it would require an increase of the computational cell and time), a different but equivalent approach is used. For example, we simulate the effect of particle size growth on its shape by gradually increasing the magnitude of the strain energy contribution at a constant particle volume. According to relation (7), it will generate the same effect on the ratio, ξ, and hence on the particle shape as increasing the particle volume during its coarsening.

Figure 3 shows the dependence of the equilibrium particle shape on ξ obtained as a result of shape relaxation during coarsening. In all the three cases examined, the particle forms a faceted rhombus. However, the detailed morphology of the rhombus depends on ξ. For example, its facets and corners are smoothly curved (Fig. 3(a)) when ξ is high and become straight and sharp as ξ decreases (Figs. 3(b) and (c)). This shape change is accompanied by an increase of the particle aspect ratio caused by rotations of the facets. If the orientation of the facets is characterized by an angle formed between the facets and the horizontal direction,[10] it is shown that this angle changes from $\sim 16°$ to $\sim 10°$ upon decrease of ξ. The latter number is very close to the value 9.4° which follows from minimizing the function $B(\mathbf{n})$ in Eq. (5) with respect to the direction $\mathbf{n}$. Qualitatively, similar rotations of the particle habits during coarsening were also predicted by Hong *et al.*[16] for the tetragonal $Fe_{16}N_2$ precipitates in cubic α iron and by Bateman and Notis[12] for tetragonal ZrO_2 in cubic ZrO_2 from an energetic analysis which incorporates the aspect ratio of a platelike precipitate into the elastic energy calculations.

The above simulation results suggest that when the interfacial energy is about the same order of magnitude as the strain energy (it corresponds to early stages of coarsening when the particles are small in size), the facets of a tetragonal particle should be diffuse and the orientation of the facets may not correspond to that predicted by the strain energy minimization. As the particles grow to larger sizes, where the strain energy contribution becomes dominant over the interfacial energy, more pronounced facets should be expected and the facet orientation could be predicted by the strain energy argument. We may call this phenomenon strain-induced faceting. This prediction is confirmed by the experimental observations by Bateman and Notis.[12] They observed a particle shape transformation from "soft" (smoothly curved) to "hard" (straight) facet during coarsening in Mg-Y PSZ.

We can roughly estimate the specific interfacial energy for Mg-PSZ by assuming that the simulated (Fig. 4(a), a reprint of Fig. 3(b)), and experimentally observed (Fig. 4(b)) particles, which are similar in shape and aspect ratio, have the same size. Dividing the total interfacial energy of the particle in Fig. 4(a) obtained from the computer simulation by its total surface area (assuming that the particle has a unit length along the third dimension), a value of 235 erg/cm^2 is obtained, which is of the same order of magnitude as the value 150 ± 50 erg/cm^2 obtained by Lanteri *et al.*[11] from a more rough estimation (from the average aspect ratio of the experimentally observed particles under an assumption that the particles have a platelike shape).

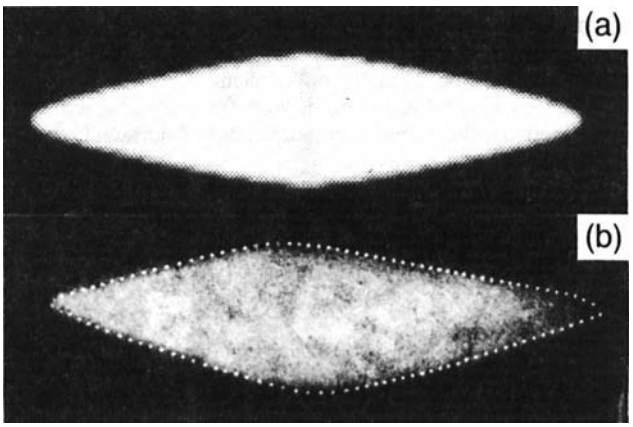

Fig. 4. Comparison between the simulated (a) and experimentally observed (b) (from Ref. 8) particle morphologies.

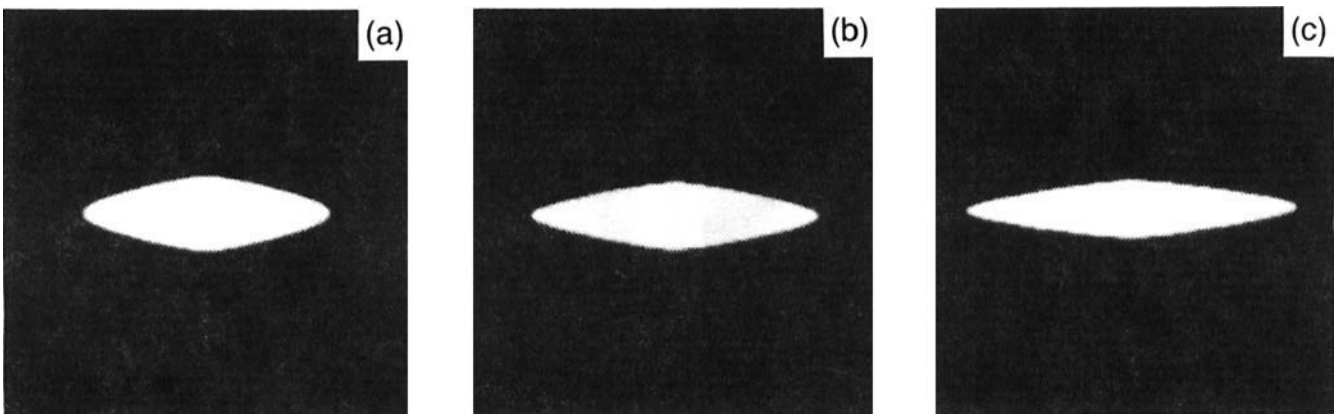

Fig. 3. Equilibrium particle shape as a function of the interfacial-to-strain energy ratio ξ. (a) $\xi = 1.05$, (b) $\xi = 0.72$, (c) $\xi = 0.57$. About 40% of the computational cell is presented.

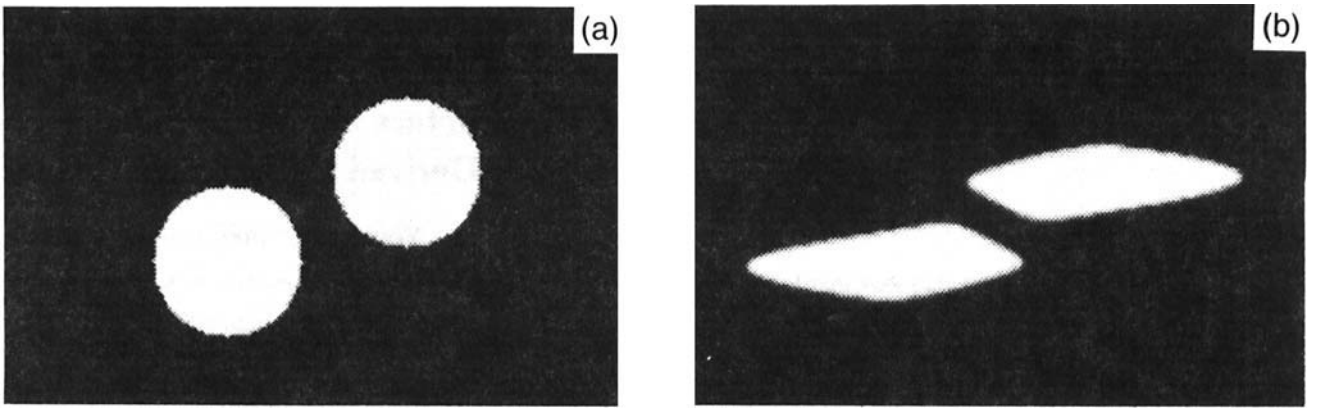

Fig. 5. Shape relaxation in a two-particle system, showing the effect of interparticle interaction on particle morphology. (a) initial configuration, (b) relaxed equilibrium configuration. About 42% of the computational matrix is presented.

The simulation results presented above do not describe the effects of strain-induced and diffusional multiparticle interactions on the particle shapes, which are actually observed experimentally.[12] For this reason, the particles obtained in our computer simulation are always symmetrical. A possible multiparticle effect is illustrated in Fig. 5 for a particular case of two interacting particles. The particles have initially a circular shape and a radius of 20 Δr (Fig. 5(a)). It can be readily seen that the evolution of the two-particle morphology leads to a structure (Fig. 5(b)) which is substantially different from those obtained in the single-particle system (e.g., Fig. 3(b)), even though the particles in both systems have faceted shapes. This simulation demonstrates that the interparticle interaction may play an important role in determining the particle shapes in a dense multiparticle system.

Acknowledgments: We are grateful to Dr. W. M. Kriven for sending us the excellent TEM pictures of t-ZrO_2 particles and for helpful discussions, and to Drs. W. R. Cannon, M. R. Notis, and C. A. Bateman for valuable discussions. The graphics are made by using the DrawCGM package developed by J. Welling at the Pittsburgh Supercomputing Center.

References

[1]V. S. Stubican, "Phase Equilibria and Metastabilities in the Systems ZrO_2–MgO, ZrO_2–CaO, and ZrO_2–Y_2O_3"; pp. 71–82 in Advances in Ceramics, Vol. 24A, *Science and Technology of Zirconia III*. Edited by S. Somiya, N. Yamamoto, and H. Yanagida. American Ceramic Society, Westerville, OH, 1988.

[2]A. H. Heuer, "Transformation Toughening in ZrO_2-Containing Ceramics," *J. Am. Ceram. Soc.*, **70,** 689 (1987).

[3]W. R. Cannon, "Transformation Toughened Ceramics for Structural Applications," *Treatise Mater. Sci. Technol.*, **29,** 195 (1989).

[4]R. H. J. Hannink, "Growth Morphology of the Tetragonal Phase in Partially Stabilized Zirconia," *J. Mater. Sci.*, **13,** 2487 (1978).

[5]D. L. Porter, A. G. Evans, and A. H. Heuer, "Transformation-Toughening in Partially-Stabilized Zirconia (PSZ)," *Acta Metall.*, **27,** 1649 (1979).

[6]D. L. Porter and A. H. Heuer, "Microstructural Development in MgO-Partially Stabilized Zirconia (Mg-PSZ)," *J. Am. Ceram. Soc.*, **62,** 298 (1979).

[7]L. H. Schonlein, "Microstructural Studies of an Mg-PSZ"; Ph.D Thesis. Case Western Reserve University, Cleveland, OH, 1982.

[8]M. Ruhle and W. M. Kriven, "Analysis of Strain around Tetragonal and Monoclinic Zirconia Inclusions"; pp. 1569–1573 in Proceedings of International Conference on Solid–Solid Phase Transformations. Edited by H. I. Aaronson, D. E. Laughlin, R. F. Sekerka, and C. M. Wayman. The Metallurgical Society of AIME, Warrendale, PA, 1982.

[9]A. H. Heuer, R. Chaim, and V. Lanteri, "Review: Phase Transformations and Microstructural Characterization of Alloys in the System Y_2O_3–ZrO_2"; see Ref. 1, pp. 3–20.

[10]A. H. Heuer and M. Ruhle, "Phase Transformations in ZrO_2-Containing Ceramics: I, The Instability of c-ZrO_2 and the Resulting Diffusion-Controlled Reactions"; pp. 1–13 in Advances in Ceramics, Vol. 12, *Science and Technology of Zirconia II*. Edited by N. Claussen, M. Ruhle, and A. Heuer. American Ceramic Society, Columbus, OH, 1984.

[11]V. Lanteri, T. E. Mitchell, and A. H. Heuer, "Morphology of Tetragonal Precipitates in Partially Stabilized ZrO_2," *J. Am. Ceram. Soc.*, **69,** 564 (1986).

[12](a) C. A. Bateman, "Aspects of Precipitation in Mg-Based Partially Stabilized Zirconias"; Ph.D. dissertation. Lehigh University, Bethlehem, PA, 1990; (b) C. A. Bateman and M. R. Notis, "Coherency Effects during Precipitate Coarsening in Partially Stabilized Zirconias," *Acta Metall. Mater.*, **40,** 2413 (1992).

[13]A. G. Khachaturyan, "Some Questions Concerning the Theory of Phase Transformations in Solid," *Sov. Phys.—Solid State*, **8,** 2163 (1967); see also the monograph *"Theory of Structural Transformations in Solids."* Wiley, New York, 1983.

[14]J. D. Gunton, M. S. Miguel, and P. S. Sahni, "The Dynamics of First-Order Phase Transitions"; pp. 267–466 in *Phase Transitions and Critical Phenomena*, Vol. 8. Edited by C. Domb and J. L. Lebowitz. Academic Press, New York, 1983.

[15]A. G. Khachaturyan and G. A. Shatalov, "Elastic-Interaction Potential of Defects in a Crystal," *Sov. Phys.—Solid State*, **11,** 118 (1969).

[16]M. Hong, D. E. Wedge, and J. W. Morris, Jr., "The State and Habit of the $Fe_{16}N_2$ Precipitate in b.c.c. Iron: Elastic Theory," *Acta Metall.*, **32,** 279 (1984). □